Optical Materials 101 (2020) 109708

Contents lists available at ScienceDirect

Optical Materials

journal homepage: http://www.elsevier.com/locate/optmat

Dopant induced modifications in the microstructure and nonlinear optical properties of 4N4MSP chalcone doped PVA films

E. Deepak D'Silva [a,*], Ismayil [b,**], Anshu Gaur [c], S. Venugopal Rao [d]

[a] Post Graduate Department of Physics, St. Philomena College, Puttur, 574202, Karnataka, India
[b] Department of Physics, Manipal Institute of Technology, Manipal Academy of Higher Education, Manipal, 576104, Karnataka, India
[c] School of Physics, University of Hyderabad, Prof. C. R. Rao Road, Gachibowli, Hyderabad, 500046, Telangana, India
[d] Advanced Center of Research in High Energy Materials (ACRHEM), University of Hyderabad, Prof. C. R. Rao Road, Gachibowli, Hyderabad, 500046, Telangana, India

ARTICLE INFO

Keywords:
PVA
Nonlinear optics
Fluorescence
Charge transfer complexes
Powder XRD
Z-scan

ABSTRACT

4M4MSP doped PVA films were prepared with dopant concentrations of 0.1, 0.25, 0.5, 0.75 and 1.0 wt% by solution casting method. From the study of FTIR spectra of the films the molecular structure was confirmed by the frequency vibrations corresponding to functional group bonding. The frequency shift in the molecular bonding establishes the possibility of formation of charge transfer complexes (CTC). UV–Visible spectra were utilized for following investigations viz: observed the shift in the absorption peaks to the higher wavelength region; decrease in the optical band gap energy from 5.02 (for pure PVA) to 2.33eV, the enhancement in the dielectric constant from 3 (for pure PVA) to 7 in the visible region; and the shift in the dielectric loss towards shorter wavelength upon increase in the dopant concentration. The studies of powder XRD spectrum explore the increase of amorphous nature of the film with the increase of dopant. From the fluorescence spectrum it is observed that fluorescence peak intensity increases up to 0.5 wt% of dopant concentration and for higher concentration it decreases. The significantly superior nonlinear absorption and refraction parameters ($\sim 10^{-10}$ cm/W and $\sim 10^{-11}$ esu, respectively) of the composite compared with pure PVA obtained from the femtosecond Z-scan technique suggests the possibility of the composite to be useful in photonics/opto-electronics applications.

1. Introduction

In recent years the development of nonlinear optical (NLO) polymer composites have gained much research interest. This is due to the fact that stabilization of dipole alignment in these composites can be achieved under electrically applied field and are useful for the fabrication of optoelectronic devices. The NLO properties of the polymer composites are mainly dependent on the composition of the composite as well as on the characteristic properties of the parent polymers. The polymers and NLO chromophores taken in an adequate quantity can lead to the enhancement of the characteristic performance of doped polymer films in an efficient manner. Also, these doped polymers are considered to be superior in-term of cost and ease of synthesis than compared with newly synthesized polymers [1]. Polyvinyl alcohol (PVA) is an artificial polymer, essentially synthesized by means of saponification method of polyvinyl acetate [2]. This polymer is widely used by the combination with other natural polymer compounds due to its film-forming ability, hydrophilic nature, and reactive high density chemical functional (–OH) groups which helps in the cross-linking of PVA with dopant compound and hence increases the mechanical properties of the films [3]. PVA polymer, offers high value of dielectric strength, superior mechanical properties and good charge-storage capacity [4]. The dopant-dependent optical and electrical properties and biocompatibility of PVA polymer have been used widely for the applications of electrochromic and electrochemical devices [5,6]. Low efficiency, lower refractive index, high cost and fast degradation rate are the main causes for the hurdles in the application of the organic polymers in other optoelectronic devices and in the solar cells [7]. According to a review article the suitable materials for practical applications should possess certain range of energy band gap usually from 1 eV to 1.7 eV. Now here does the need arise to tailor the wide-band gap (5.02 eV) PVA polymer into a small band gap and good film forming material [8]. Organic molecules particularly chalcones are considered to be superior over inorganic molecules for the applications in the field of nonlinear optics (NLO) [9]. The electronic

* Corresponding author.
** Corresponding author.
E-mail addresses: deepak@spcputtur.org (E.D. D'Silva), ismayil.mit@manipal.edu (Ismayil).

https://doi.org/10.1016/j.optmat.2020.109708
Received 2 December 2019; Received in revised form 7 January 2020; Accepted 18 January 2020

charge distribution is delocalized in chalcone which has the π-conjugated molecular system. Therefore, the electron density in the chalcone has the high mobility [10]. The suitable electron donating or accepting groups situated at appropriate positions on the aromatic rings of the chalcone may cause asymmetric distribution of electrons either in the ground state or excited state or in the both states. This asymmetric distribution of the electrons increases the molecular hyperpolarizability and the ability to crystallize [11,12]. Chalcones are organic molecules having π-conjugated system exhibiting promising linear and non-linear optical properties are extensively studied for their applications in non-linear optical materials. The nitro group substituted at the para position of the aromatic ring of the chalcone (2E)-3-[4-(methylsulfanyl) phenyl]-1-(4-nitrophenyl)prop-2-en-1-one (4N4MSP) shows high second order harmonic generation (SHG) efficiency, which is almost 28.57 times more compared with that of urea and significant third order nonlinear optical properties [13]. The NLO materials have many applications such as in the field of optical signal processing, optical computers, ultrafast switches, ultra-short pulsed lasers, sensors, optical limiters, laser amplifiers, and many others [12]. This paper includes the discussion on the preparation of novel nitro substituted chalcone 4N4MSP doped PVA polymer composite films and to study the possible application of these films in non-linear optics (NLO) as well as in high energy conversion efficient solar cells.

2. Experimental methods

The solution casting method was used to prepare dopant induced PVA films. The PVA films with different concentration of 4N4MSP dopant (0.1, 0.25, 0.5, 0.75, 1.0 wt%) were prepared by solution casting method. PVA polymer powder was added to 50 ml of N, N, dimethyl formamide and allowed to swell the particles with stirring the solution at 45 °C temperature. Necessary quantities of dopant 4N4MSP were also dissolved in the same solvent and transferred to the polymeric solution while stirring. The solution was poured on to a clean Petri dish and was dried at room temperature. The films were then peeled from the plate, after drying. The thickness of the prepared films was measured using Mitutoyo-7327 dial thickness gauge and the obtained values for our samples were in the range of 250 μm–350 μm. The absorption spectra of the composite films were taken at wavelengths ranging from 200 nm to 800 nm using Shimadzu UV-1800 spectrophotometer. The FTIR spectrum of the samples was recorded by Bruker Advance III, 400 MHz spectrophotometer in the 400–4000 cm^{-1} wave number range. The fluorescence emission spectrum (steady state) was recorded by exciting the sample at its absorption wavelength of 428 nm using Jobin Yvon Fluorolog-3-11 spectrofluorometer. In the present study the powder X-ray diffraction graphs of the present materials were obtained by a Bruker AXS D8 Advance X-ray diffractometer with nickel K_β filter and CuK_α radiation of wavelength $\lambda = 1.5406$ Å was used with a graphite monochromator. The nonlinear absorption and refraction studies were performed by the standard Z-scan technique at 800 nm using a pulsed laser beam from Ti: Sapphire Laser (M/s Coherent) of pulse width ~50 fs and pulse repetition rate of 1 kHz.

3. Results analysis and discussion

3.1. Study of FTIR spectrum

The FTIR spectra of pure and 4N4MSP doped PVA sample films prepared with different doping concentrations are shown in Fig. 1. It is seen from the FTIR spectrum of pure PVA that hydroxyl (O–H) stretching groups of PVA can be revealed as a peak at 3416 cm^{-1}. The vibrations corresponding to 2926 cm^{-1} and 2849 cm^{-1}, respectively, represent the C–H asymmetric stretching and symmetric stretching. The methyl group indicated by C–H bending is represented by the peak at 1426 cm^{-1}. The PVA main chain having the acetyl group is shown as C–O stretching has the peak vibration at 1085 cm^{-1}. The C═C stretching vibrations

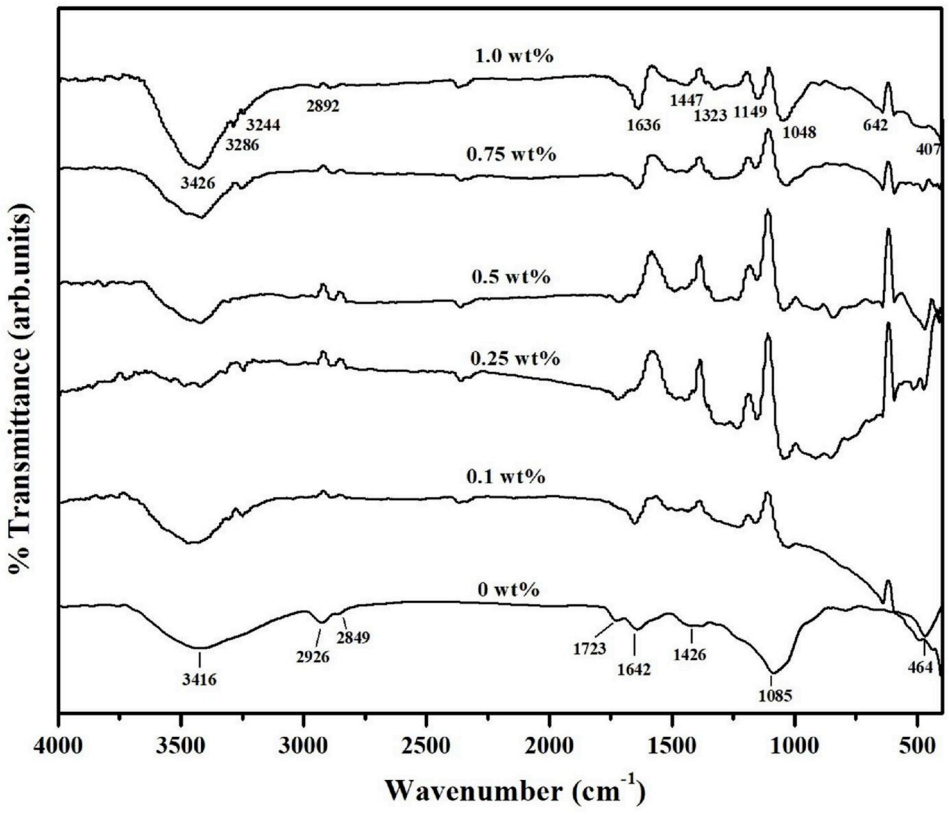

Fig. 1. FTIR spectra of pure and 4N4MSP doped PVA composite films.

represented by faint absorption peaks occur around 1642 cm^{-1} and the vibrations around 1723 cm^{-1}corresponds to acetylic C═O stretching. The bending and wagging vibrations corresponding to CH_2 group are observed respectively at 1426 cm^{-1} and 1323 cm^{-1} [14].

Upon observing the 4N4MSP/PVA spectrum of the polymer samples, it is noted that the C–H stretch (asymmetric) corresponding to pure PVA at 2926 cm^{-1} has moved to 2892 cm^{-1} (1 wt%) after doping with 4N4MSP. The frequencies 1642 cm^{-1}corresponding to stretching of C═C of PVA have moved to 1636 cm^{-1}. The O–H (hydroxyl) groups of pure PVA at frequency 3416 cm^{-1} have been moved to 3426 $cm^{-1}$for the doped films of different concentrations. These shifts in the frequency of vibrations suggest the presence of intense interaction of 4N4MSP with PVA leading to form a charge transfer complex (CTC). The complete understanding of this can be drawn from the study of hydrophobic interaction and hydrogen bonding between PVA and 4N4MSP according to the reaction scheme as shown in Fig. 2.

The methylthio (SCH_3) as well as the $–NO_2$ groups interaction of chalcone 4N4MSP with the PVA O–H groups in the PVA/4N4MSP composite is anticipated to be taking place at different PVA main chain positions [15]. The hydrogen bonding (as in the reaction mechanism) between the 'S' atom of methylthio group and 'N' atom of $–NO_2$ group of 4N4MSP with O–H group of the polymer is the reason for the formation of CTC. This causes the increase in the population or electron density of the antibonding orbital of O–H. Thus, the increase of population weakens the O–H bond, so elongation of the bond takes place and thus restricts the shift of O–H stretching frequency. The hydrophobic interactions represented by Fig. 2(b) also occur. The peak vibrations are presented in Table 1.

3.2. Study of UV–Visible spectrum

The optical ultraviolet visible absorption spectra of pure PVA and doped 4N4MSP PVA films are illustrated in Fig. 3. The absorption spectrum of PVA/4N4MSP composites show shift in the absorption edge against the spectrum of pure PVA. Here one can observe the red shifted absorption edge of pure PVA at ca. 245 nm to ca. 475 nm for 1 wt% 4N4MSP doped composite film. Further, the absorbance is observed to be increasing with the increase of dopant concentration. This implies that the incorporation of organic compound into the polymer matrix has formed extra energy levels within the optical energy band gap. The hydrogen bonding between –OH group of PVA with $–NO_2$ and $–SCH_3$ groups of 4N4MSP introduces additional energy levels and lead to the formation of CTC as also evident from FTIR results. The making of novel molecular dipoles or the reorientation of old dipoles takes place because of the creation of CTC. As observed from FTIR studies, the buildup of the polar functional groups upon doping lead to the formation of point defects. The point defects created within the band gap is also the reason for the formation of molecular dipoles. The formation and accumulation of these dipoles inside the optical band gap results in the creation of point defects will change the microstructure of the polymer and due to this there is red shift in the absorption edge. The modification in the NLO activity of the polymers is due to the formation or reorientation of these dipoles. The clarity on the electronic band structure of polymeric materials can be obtained through the study of the optical absorption coefficient. Using absorption spectra, the absorption coefficient α was determined by the relation [16],

$$\alpha = \frac{2.303\,A}{t} \tag{1}$$

Table 1
The FTIR peaks assignments of PVA/4N4MSP polymer composite films.

Wave number (cm^{-1})		Peak assignment
PVA	PVA/4N4MSP	
3416	3426	O–H stretching
2926	2892	C–H asymmetric stretch (alkyl)
2849	2849	C–H symmetric stretching
1723	1723	C=O stretching vibrations
1642	1636	C=C/C=N stretch
1426	1447	C–H bending
1323	1323	C–H wagging
–	1149	C–C rocking vibration
1085	1048	C–O stretch, C–H and O–H bend
464	407	Out of plane vibrations

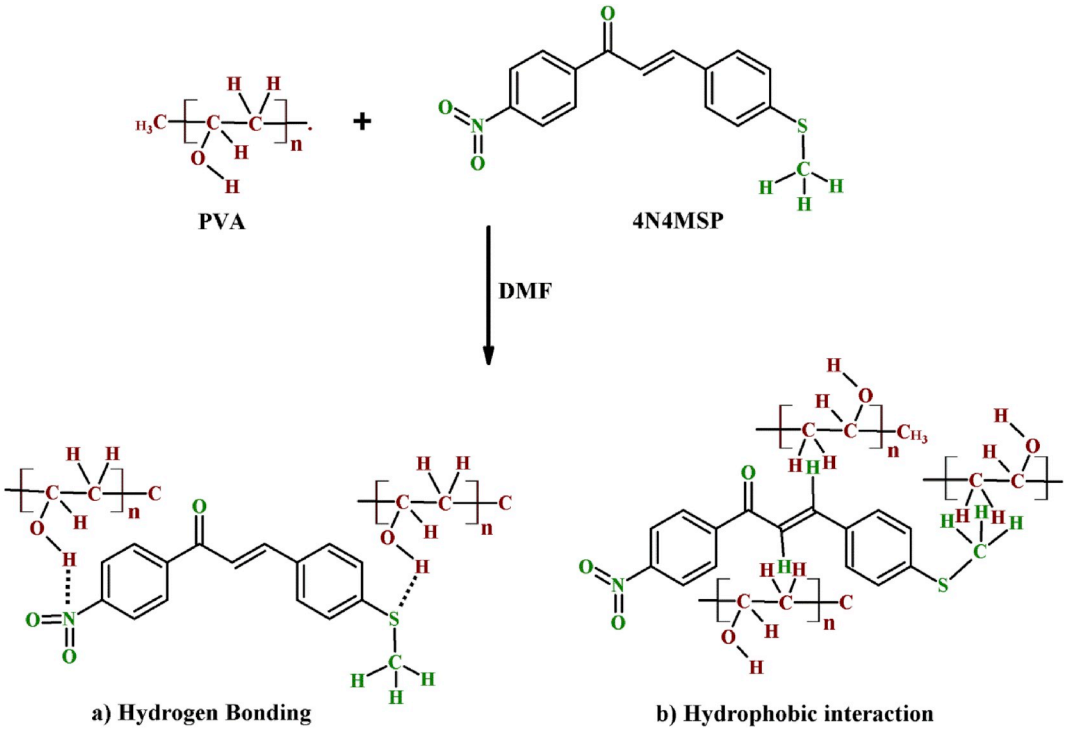

Fig. 2. Reaction scheme of a) Hydrogen bonding and b) Hydrophobic interaction of PVA with 4N4MSP.

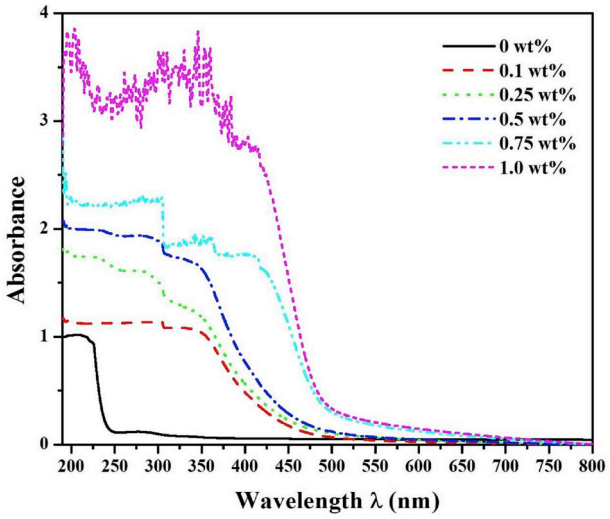

Fig. 3. The UV–Visible spectrum of pure and 4N4MSP doped PVA polymer composite films.

where *A* represents the absorbance, *t* is the sample thickness. The optical band gap energy E_g of the pure PVA and PVA/4N4MSP films were calculated by Tauc's plot [17];

$$\alpha h\nu = B\left(h\nu - E_g\right)^m \tag{2}$$

where B is an energy independent constant and *m* is an index whose value is determined by the indirect allowed transitions and is given by m = 2. The plot between $(\alpha h\nu)^{½}$ versus hν at ambient temperature represents a linear behavior, which is the confirmation for the indirect allowed transition for pure PVA and PVA/4N4MSP films and are represented by the plots given in Fig. 4. The E_g value of pure PVA is found to be 5.02 eV.

It is observed from Fig. 4 that optical band gap values of doped PVA are less compared with the pure PVA [18]. These changes in the E_g values of 4N4MSP doped PVA films validate the modifications in the PVA microstructure and band structure, because of the creation of additional groups for optical transitions. Using Urbach formula $\alpha = \alpha_0 \exp(h\nu/E_u)$, the Urbach energy E_u, which is a parameter representing optical transitions mechanism, is estimated [19]. In order to calculate Urbach energy, the graph of ln α (natural logarithm of the absorption coefficient) versus photon energy 'hν' was plotted and reciprocal of the slope of the straight line in the linear region of the plot was determined (Fig. 5).

It is seen that the value of E_u for pure PVA is 0.3eV and as the doping concentration increases E_u value increases. The values of optical band gap energy and Urbach energy are presented in Table 2. The mobility concept of Davis and Mott [20,21] is helpful to understand decrease or increase of E_u values in pure and doped PVA. The cluster groups within the composite increases as the concentration of 4N4MSP increases. These cluster groups ensuing in the creation of dopant aggregates or agglomerates, enhances the imperfect structures within the doped samples. The defective structures thus formed might have introduced extra energy states inside the optical band gap. Therefore, the presence of defects will change the charge distribution and electronic levels in the vicinity of defects. Thus, the presence of defects causes the decrease of optical band gap energy values with the increase of the doping level and also increase in the Urbach energy. The fraction of electromagnetic energy lost due to the scattering and absorption per unit thickness in a particular medium is given by extinction coefficient (k) and was calculated for the materials by the equation [22];

$$k = \frac{\alpha\lambda}{4\pi} \tag{3}$$

where λ and α represents the wavelength and the absorption coefficient of the given material respectively. Fig. 6 shows the variation of the refractive index (*n*) of pure and 4N4MSP doped PVA polymer composite films versus wavelength. Using Fresnel formula [23] the refractive indices of the films were estimated from the parameters reflectance (R) and extinction coefficient (k),

$$n = \frac{(1+R)}{(1-R)} + \sqrt{\frac{4R}{(1-R)^2} - k^2} \tag{4}$$

The complex dielectric constant is the inherent property of a material. The real part of complex dielectric constant shows that materials having high value of the refractive index can effectively reduce the speed of light, whereas the imaginary part gives the information about the absorption of energy from an electric field by the dielectric medium due to dipole motion. As refractive index increases more strongly the light is slowed down. The real and imaginary parts of the dielectric constant can be calculated by below given expressions [24];

$$\varepsilon' = n^2 - k^2 \text{ and } \varepsilon'' = 2nk \tag{5}$$

Figs. 7 and 8 stand for real and imaginary parts of the complex optical dielectric constant of the pure and 4N4MSP doped PVA polymer

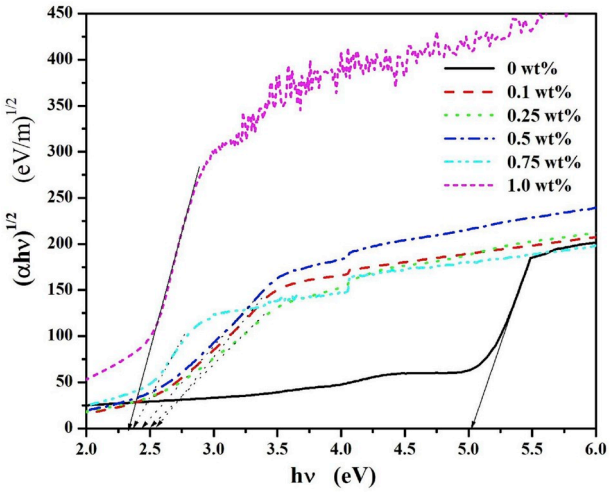

Fig. 4. Graph of $(\alpha h\nu)^{½}$ versus photon energy for pure and 4N4MSP doped PVA polymer composite films.

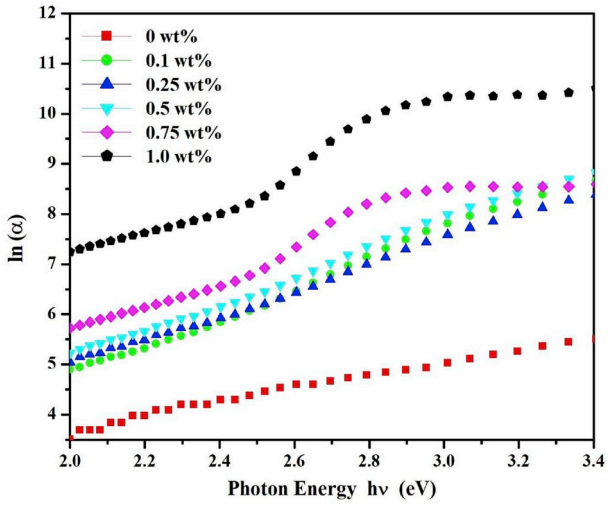

Fig. 5. Graph of ln(α) versus photon energy for pure and 4N4MSP doped PVA polymer composite films.

Table 2
The optical band gap energy and Urbach energy of PVA/4N4MSP polymer composite films.

Dopant Concentration	Optical band gap energy (eV)	Urbach energy (eV)
Pure PVA	5.02	0.78
0.1 wt %	2.60	0.50
0.25 wt%	2.53	0.39
0.50 wt%	2.46	0.36
0.75 wt%	2.38	0.22
1 wt%	2.33	0.18

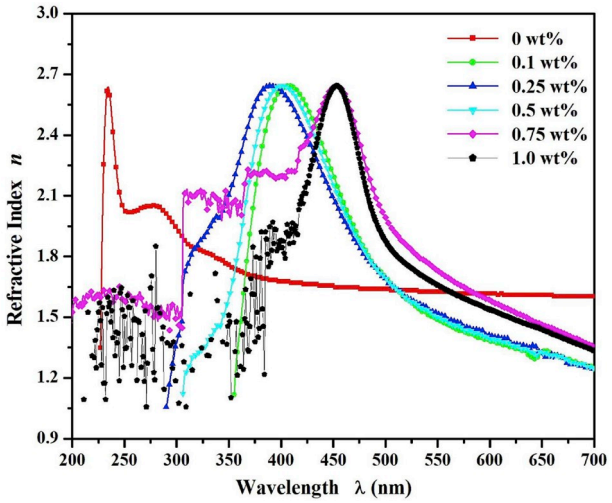

Fig. 6. Refractive index (n) of pure and 4N4MSP doped PVA polymer composite films versus wavelength.

composite films. From Figs. 7 and 8 one can observe that the values of the real part (Fig. 7) are high compared with the imaginary part (Fig. 8). From Fig. 7 it can be seen that the dielectric constant of the pure PVA in the visible region is around 3 and it enhanced to around 7 upon doping. The dielectric constant is directly related to the density of states within the energy band gap, therefore the enhancement of the dielectric constant in the visible wavelength region upon doping can be attributed to the rise in the density of states [25]. Fig. 8 shows that the peaks corresponding to dielectric loss shift to shorter wavelength or towards higher

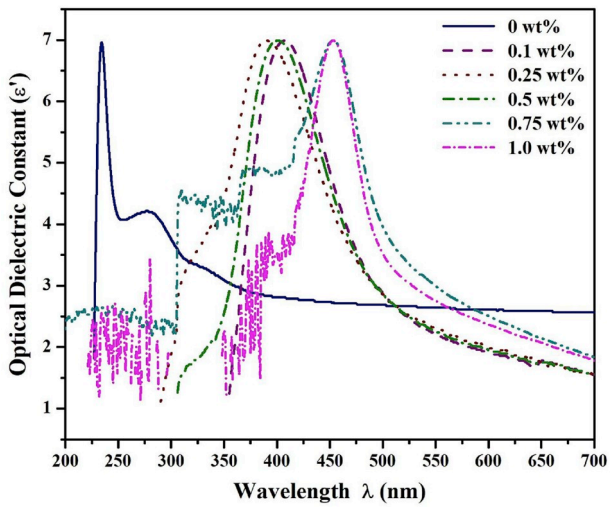

Fig. 7. Optical dielectric constant versus wavelength for pure and 4N4MSP doped PVA polymer composite films.

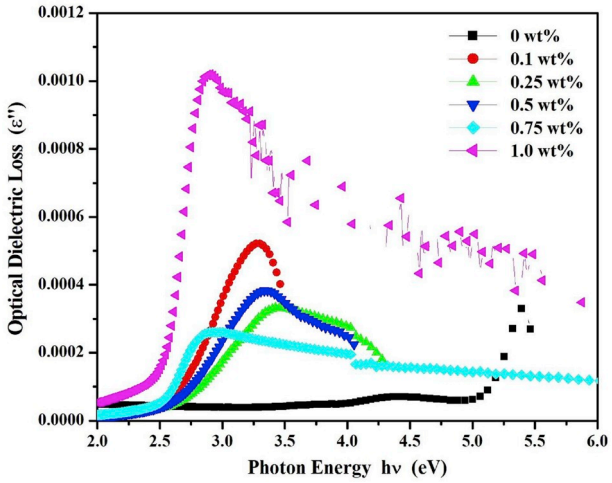

Fig. 8. Optical dielectric loss as a function of photon energy for pure and 4N4MSP doped PVA polymer composite films.

frequency with respect to the increase in the concentration of 4N4MSP addition. It is also observed that the real part of the optical dielectric constant and also the imaginary part exhibit a dispersion behavior with wavelength. The materials which show dispersion behavior as stated are useful in designing the optical devices which are especially utilized in optical communication applications [26].

3.3. X-ray diffraction studies

The modifications in the microstructure of PVA due to the doping of 4N4MSP are inspected through X-ray diffractogram (XRD). The XRD pattern of pure and 4N4MSP doped PVA films are shown in Fig. 9. The pattern shows a comparatively sharp and wide peak centered on $2\theta = 20.08^{\circ}$ and a small peak at $2\theta = 40.9^{\circ}$ designates that polymer PVA has both crystalline and amorphous phase (semi-crystalline nature). Small crystallites are randomly distributed in the crystalline phase whereas free volumes are filled with amorphous phase of the PVA matrix [14]. It is observed that the area under the peak decreases for 4N4MSP doped PVA, implies that amorphous nature of the film increases with dopant concentration. This amorphous character of the film causes the formation of cross-linking network within the polymer matrix through inter and intra molecular interactions and produce the polymer complex with the dopant [27]. A slight broadening of the X-ray peak upon doping affirms point defects or poor crystallinity of the films. Increase in the amorphous nature of the film can be correlated with the decrease in the Urbach energy, which is a measure of molecular ordering.

In the complex structure 4N4MSP compound may get into and dwell in the core lattice sites of the polymer chains by linking them with the hydrogen bond through the charge transport processes. Thus, the structural repositioning within the polymer matrix occurs as the amorphous nature increases. Hence, it is clear that through the hydrogen bonding of hydroxyl groups of the polymer side chain with the dopant 4N4MSP compound (also evident from FTIR spectra) ensure a major role on the charge mobility within the chain and on the structure of the polymer. The parameters related to the infrastructure of films such as crystallite size, micro-strain and dislocation density have also been estimated from XRD spectra. From Scherrer formula [28], crystallite size (D) is given by,

$$D = \frac{0.9\lambda}{\beta \cos\theta} \tag{6}$$

where β is FWHM of the diffraction peak, λ is the wavelength of the X-ray source, and θ is Bragg angle. Micro-strain (ε) and dislocation density (δ) of the films are calculated using the formulae $\varepsilon = (\beta\cos\theta)/4$ and $\delta = 1/D^2$

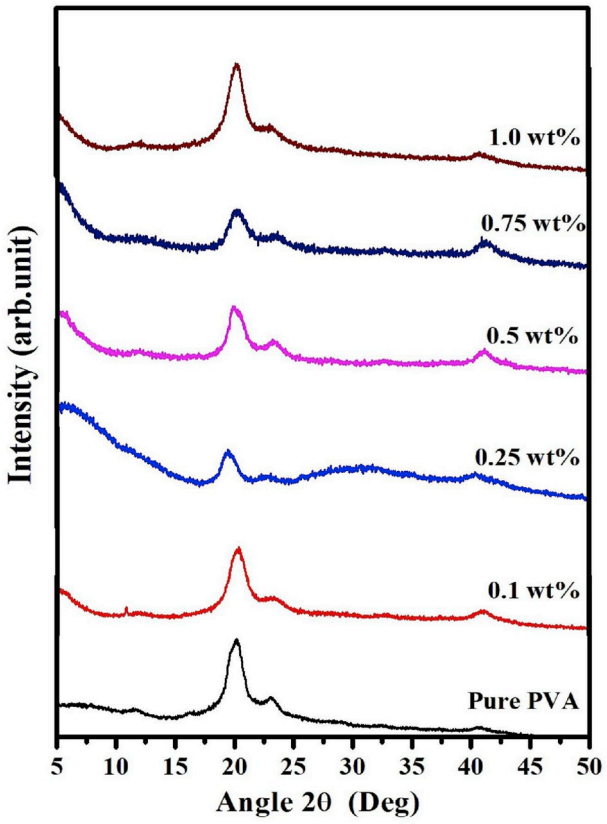

Fig. 9. XRD spectra of pure and 4N4MSP doped PVA polymer composite films.

respectively. The obtained values are presented in Table 3.

3.4. Fluorescence studies

The fluorescence spectra of the 4N4MSP doped PVA polymer composite films are shown in Fig. 10 [29]. When the emission spectrum of the donor component and the absorption spectrum of the acceptor are overlapping with each other and the dipoles are sufficiently close to each other causes the energy transfer in the composite film. PVA in its pure form do not give any fluorescence effect and therefore the fluorescence recorded for the doped materials as shown in Fig. 10 is due to the presence of 4N4MSP chromophore. From the figure it is observed that fluorescence emission peak wavelengths shift to the lower wavelength region where as the intensity of fluorescence emission is increasing with the doping of 4N4MSP. The composite PVA/4N4MSP is giving an excellent fluorescence spectrum.

The chalcone crystal (4N4MSP) structure has electron donating (SCH_3) and electron accepting group (NO_2) attached to its aromatic rings to form donor-π acceptor-π-acceptor (D-π-A-π-A) type of the molecule. Therefore, the effective system is a D-π-A systems and charge

Table 3
Analysis of XRD data of 4N4MSP doped PVA polymer composite films.

Dopant Concentration wt%	2θ (deg)	d-spacing (Å)	Crystallite size D (Å)	Micro-strain ε	Dislocation density δ ($\times 10^{20}$) (m^{-2})
0	20.11	4.41	0.505	0.685	3.91
0.1	20.18	4.39	0.525	0.659	3.61
0.25	19.47	4.55	0.786	0.440	1.61
0.5	19.89	4.45	0.690	0.501	2.09
0.75	20.20	4.39	0.640	0.541	2.43
1	20.19	4.39	0.513	0.674	3.78

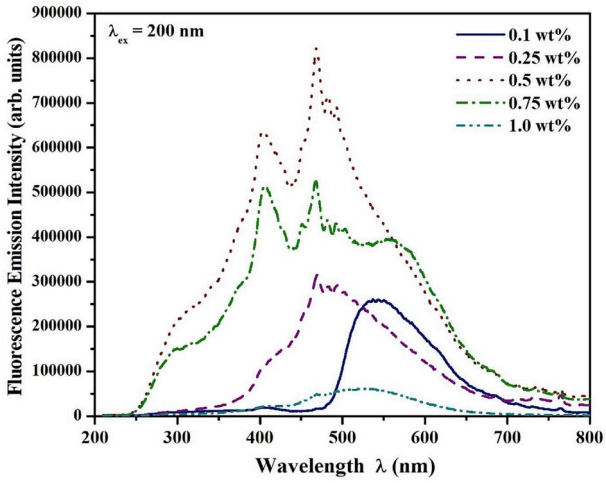

Fig. 10. Fluorescence emission spectra of4N4MSP doped PVA polymer composite films.

transfer path is from donor to acceptor. In the crystal system of 4N4MSP all oxygen atoms present in the molecule are involved in intermolecular bonding with neighboring 4N4MSP molecules. The intermolecular hydrogen bonds between polymer and the dopant group tie up the nonbonding electron pairs within 4N4MSP group and allow the fluorescence to occur. The intramolecular charge transfer within 4N4MSP, the intermolecular hydrogen bonds between PVA and 4N4MSP responsible for the creation of CTC and thus depict fluorescence [30].

The data shows fluorescence emission wavelength (λ_{max}) shifted from 545 nm to 470 nm for 200 nm excitation wavelengths. The photo generated charge species stabilized at different extents in the excited state may be the reason for the observed blue shifted emission. In the graph it can be seen that fluorescence peak intensity increases up to 0.5 wt% of dopant concentration and for higher concentration of dopant it decreases. At lower dopant concentration the molecules having π-bonds undergo successive isomerization and change their orientation, upon excitation with polarized light. Hence dipole-dipole interactions due to the aggregation of chromophores, increases the fluorescence intensity at the lower dopant concentration [31]. The molecular aggregates of 4N4MSP may cause the decrease in fluorescence emission (quenching) intensity at higher dopant concentration. The excitation energy transfer between the aggregates and monomers, and further non-radiative decay of this energy may be the reason for quenching process or decrease in fluorescence emission intensity at higher dopant (above 0.5 wt%) concentration [32].

3.5. Third order nonlinear properties

To study the third-order NLO properties of PVA doped with 4N4MSP a single beam Z-scan technique which readily provides the magnitude and sign of nonlinearity was employed [33,34]. In the experimental arrangement, a pulsed laser beam [M/s Coherent; pulse width: 50 fs (fs), repetition rate: 1 kHz] of wavelength of 800 nm with initial spot radius of 1.1 mm (closed aperture) and 1.5 mm (open aperture) was focused by using a 17 cm focal length plano-convex lens. The resulting beam waist radius (w_0) at the focus was calculated to be ~39.4 and ~28.9 μm ($=f\lambda/\pi w_i$), and Rayleigh lengths ($z_R = \pi w_0^2/\lambda$) were estimated to be 6.09 and 3.27 mm, respectively. The sample was translated along the beam direction (considered as Z-axis) on either side of the focal point and the transmitted power is measured as a function of the sample position with respect to the focal point through a photodiode (Si photodiode, SM1PD2A, Thorlabs). While traversing the z-coordinate the sample experiences the intensities given by the relation $I_z = I_{00}/[1+(z/z_R)^2]$ where I_{00} is the on-axis peak intensity at the focus. For measuring the nonlinear

(NL) refractive property, an aperture was placed in front of the photodiode (closed aperture configuration) whereas to estimate the NL absorption characteristics, the sample transmittance is recorded without the aperture (open aperture configuration).

For a temporal Gaussian pulse with an incident Gaussian spatial profile, the on-axis transmittance of 0.5 and 1.0% 4N4MSP doped PVA thin layers as a function of sample position for an input irradiance of 10 MW/cm^2 is shown in Fig. 11(a). The transmittance presented in the graph is the output (transmitted) power at the NL regime normalized with respect to the output power at the linear regime. Thus, the transmittance of 1 conveys that the sample does not show NL behavior and the transmittance of value less (greater) than 1 represents the situation when the sample transmits lesser (more) or absorbs more (lesser) than that at the linear response. In Fig. 11(a), transmittance of 0.5 and 1.0 wt % Chalcone doped PVA layer decreases with the increase of the laser intensity when the sample moves towards the focus. It happens for the sample absorption (thus transmittance) shows NL behavior and increases (decreases) with the light intensity, thus, representing RSA (reverse saturable absorption) or optical limiting characteristics. Also, the absorption gets enhanced with doping concentration which indicates the nonlinearity to be due to the dopants, at least in part. To extract/assess the contribution of the PVA host matrix in the NL behavior of the composite or doped system, the Z-scan experiment is performed on pure PVA sample and the associated graph for a higher input irradiance of 23 MW/cm^2 is presented in Fig. 11(b). Pure PVA has weak nonlinear absorption (NLA) characteristics since the decrease in the NL transmittance is lesser, for the same reason the open aperture graph is shown for higher input irradiance. The doped PVA layer exhibited a deeper valley

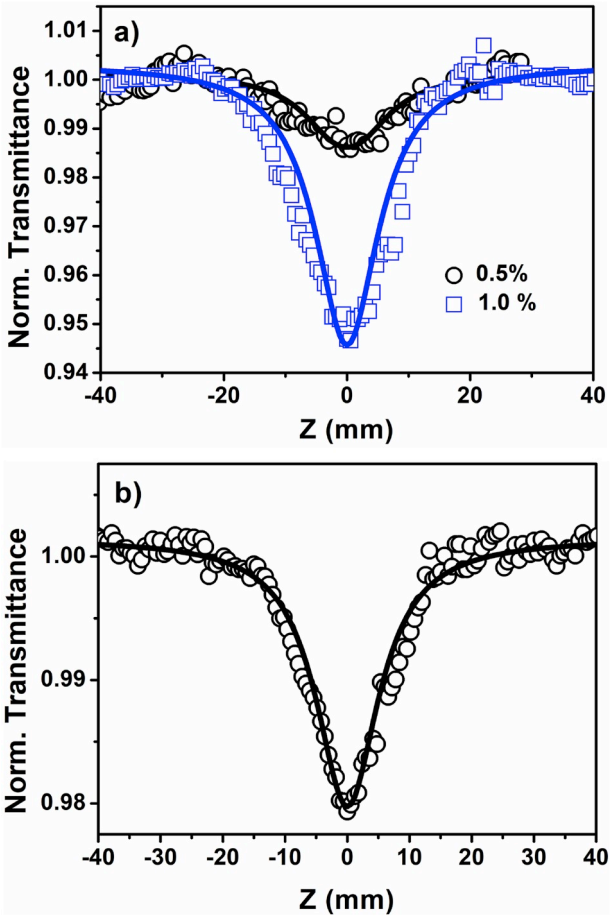

Fig. 11. Open Aperture Spectra of a) 0.5 and 1% Chalcone doped PVA at 10 MW/cm^2 and b) PVA matrix at 23 MW/cm^2. Experimental data are represented by symbols whereas fitted data are shown by solid lines.

indicating a higher nonlinearity in the absorption characteristics. The normalized transmission of PVA matrix at the higher input irradiance of 23 MW/cm^2 is almost the same (0.98) compared to that at 10 MW/cm^2 for 0.5% doping (0.985) and smaller than that for 1% (0.945). Such intensity dependent transmittance decrease behavior of the doped (and pure) PVA layers is associated with multi-photon (two-photon) absorption [35]. Since pure and doped PVA samples are weak at absorbing single photon at 800 nm wavelength (Fig. 3), the possibility of excited state absorption is discarded for being insignificant.

To estimate the NLA parameters the Z-scan data of pure and doped PVA thin layers are fitted by solving the differential equation [33],

$$\frac{dI}{dz'} = -\alpha(I)I \tag{7}$$

for the transmitted intensity I through the sample of thickness L. In Eq. (7), z' is the sample's thickness co-ordinate with respect to the origin at the laser incidence surface of the sample and $\alpha(I)$, the total absorption coefficient, given as [36,37],

$$\alpha(I) = \frac{\beta_{0PVA} I}{1 + \left(\frac{I}{I_{SPVA}}\right)^2} + \frac{\beta_{0Chalcone} I}{1 + \left(\frac{I}{I_{SChalcone}}\right)^2} \tag{8}$$

where β_{0PVA} and $\beta_{0Chalcone}$ are the two-photon absorption (2 PA) coefficients of PVA matrix and the dopant (chalcone) system respectively, I_{SPVA} and $I_{SChalcone}$ are the corresponding 2 PA saturation intensities of the matrix and the dopant system. In case of $I \ll I_{SPVA}$, i.e. negligible saturation effect in PVA, Eqn. (2) reduces to a simpler form,

$$\alpha(I) = \beta_{0PVA} I + \frac{\beta_{0Chalcone} I}{1 + \left(\frac{I}{I_{SChalcone}}\right)^2} \tag{9}$$

The same form or simplification can be applicable to the second part also when dopant system has insignificant absorption saturation. The nonlinear absorption (NLA) coefficient was determined by fitting the experimental open aperture Z-scan data by solving Eq. (1) in the MATLAB software and the obtained values are reported in Table 4. Theoretical fit of the experimental data yielded NLA coefficient β_0 (at the input irradiance of $I_0 = 10$ MW/cm^2) for pure PVA as 0.8×10^{-11} cm/W and for 0.5 and 1 wt% doped chalcone as 0.2×10^{-10} cm/W and 1.2×10^{-10} cm/W respectively. The observation of increased NL absorption of doped film compared to the pure PVA matrix is thus justified in the larger β_0-value. The reason for the increased NLO activity in the 4N4MSP doped polymer is due to the presence of SCH_3 chromophore and nitro group (-NO_2) which interacts with OH groups of PVA and forms a CTC (charge transfer complex). In the case of 4N4MSP, SCH_3 is an electron donor group and the NO_2 group is a strong acceptor group and the molecule is acceptor-acceptor-donor (A–A–D) type. In the case of A–A–D type of molecules charge transfer takes place through acceptor end to donor end (between two end groups of the molecules). The nonlinearity is related to the degree of charge transfer from the donor to

Table 4
Summary of NLO coefficients obtained from the open aperture Z-scan data of pure and Chalcone doped PVA.

Sample	Input Intensity MW/cm^2	β_{0PVA} cm/W	$\beta_{0Chalcone}$ cm/W	$I_{SChalcone}$ W/cm^2
0.5 wt% doped PVA	10	0.8×10^{-11}	0.2×10^{-10}	3.9×10^{10}
1 wt% doped PVA	10	0.8×10^{-11}	1.2×10^{-10}	3.9×10^{10}
	15	1.15×10^{-11}	2.1×10^{-10}	3.8×10^{10}
	23	1.35×10^{-11}	3.95×10^{-10}	3.6×10^{10}

the acceptor, which is in turn linked to the bond-length alternation. This charge transfer will increase the magnitude of the dipole moment and thus induces large NLO effects.

The knowledge of the dependence of transmittance on the input irradiance gives the information about the mechanism of the NLA. If slope of natural logarithmic of $(1\text{-}T_0)$ versus natural logarithmic of input irradiance is 1 (2) absorption is governed by 2 PA (3 PA) where T_0 is the sample transmittance at the focus [35,38]. Furthermore, it suggests the intensity range which can be used for optical limiting application. Irradiance dependent open aperture Z-scan graph of 1 wt % chalcone doped PVA is shown in Fig. 12. With the increase of the input irradiance from 10 MW/cm^2 to 23 MW/cm^2 the RSA characteristics is maintained; transmittance of the doped PVA sample systematically decreases for a greater number of molecules taking part in the absorption process. Slope of 1.29 of $\log_e(1\text{-}T_0)$ versus $\log_e I_{00}$ indicates the existence of 2 PA process for the observed nonlinear absorption Z-scan curves.

The normalized transmittance can be expressed by the equation for closed aperture configuration when the far-field condition $d \gg z_R$ is satisfied. Here d is the distance between the sample and the aperture plane. The typical Z-scan data with fully open aperture is not sensitive to nonlinear refraction (NLR) and data are to be symmetric with respect to the focus. But the closed aperture transmittance is affected by both NLR as well as absorption. The NLA effect can be avoided/eliminated by choosing sufficiently low input irradiance when NLA is insignificant. Otherwise the refraction part can be extracted by dividing the closed aperture transmittance data by the corresponding open aperture data [33]. The closed aperture normalized transmitted power data observed at low input power (pure NLR characteristics) for the PVA matrix and the composite (1 wt%) is shown in Fig. 13(a–b).

The valley followed by a peak in the closed aperture Z-scan graph indicates that the sign of the refraction index nonlinearity is positive (i.e., self-focusing) whereas opposite scenario of valley followed by a peak corresponds to de-focusing refraction characteristics and negative index of refraction. By the doping of chalcone, the refraction characteristics of PVA is transforming from focusing to defocusing. The nonlinear refraction coefficient, γ, was calculated by theoretical fit of equation given in the literature [33] to the experimental data. For 1% Chalcone doped PVA γ is calculated to be -2.85×10^{-14} cm^2/W whereas for pure PVA it is 5.52×10^{-14} cm^2/W. The third-order nonlinear refractive index $n_2 = [cn_0/40\pi]\gamma$ was found to be of the order -0.743×10^{-11} esu for doped PVA and 1.238×10^{-11} esu for PVA matrix. Here the value of n_0, the linear refractive index of pure PVA was taken 1.48. The calculated parameters of nonlinear absorption and refraction are found to be superior to the values reported for chalcone PDAC doped in PVA and also pure chalcone 4N4MSP reported in the literature [39,40]. Taking

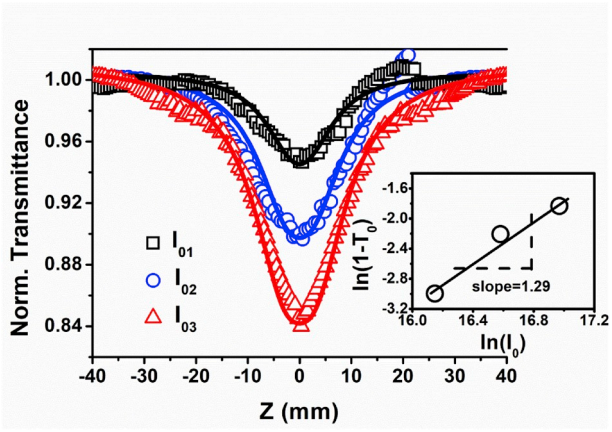

Fig. 12. Open aperture Z-scan graph of 1 wt% chalcone doped PVA at $I_{01} = 10$ MW/cm^2 (□), $I_{02} = 15$ MW/cm^2 (o) and $I_{03} = 23$ MW/cm^2 (Δ). Experimental data are represented by symbols whereas fitted data are shown by solid lines.

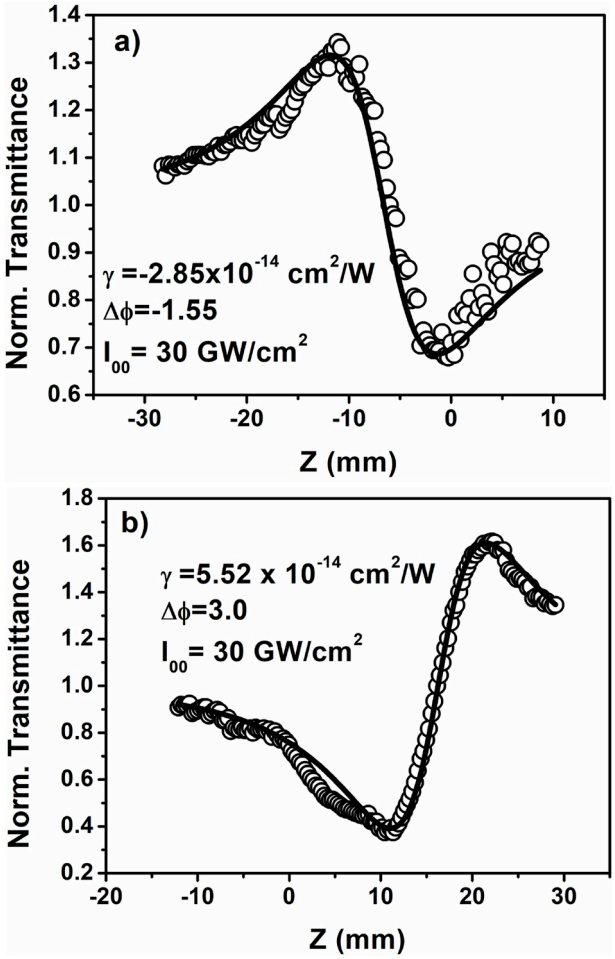

Fig. 13. The closed aperture Z-scan data of a) 1 wt% doped PVA and b) Pure PVA. Z-scan experimental data is represented by open circle and solid line corresponds to the fitted data.

into account the calculated NLR coefficient (γ) and NLA coefficient (β) the real and imaginary parts of the third-order nonlinear susceptibility can be evaluated using the relations $Re\chi^{(3)} = 2n_0^2\varepsilon_0 c\gamma$ and $Im\chi^{(3)} = n_0^2\varepsilon_0 c\lambda\beta/2\pi$[33]. Here c is the velocity of the light in vacuum, ε_0 is the permittivity of the free space, and n_0 is the linear refractive index of the sample solution. The calculated real part of third-order susceptibility $Re\chi^{(3)}$ and imaginary part $Im\chi^{(3)}$ are summarized in Table 5.

Further, origin of nonlinearity in the NLR characteristics can be confirmed by observing other features of the closed aperture Z-scan data. For example, in closed-aperture Z scan curves the distance between peak and valley (peak–valley separation), ΔZ_{p-v}, reflects the origin of the NLO process [33]; if ΔZ_{p-v} equals $1.7z_R$ and $1.2z_R$ corresponds to third-order and fifth order NLO processes, respectively. In the present

Table 5
Summary of non-linear parameters obtained in the present work for pure and Chalcone doped PVA.

Sample	Phase shift $\Delta\Phi_0$	$\gamma = \frac{\Delta\phi_0\lambda}{2\pi I_{00}L_{eff}}$ cm^2/W	$n_2 = \frac{cn_0}{40\pi}\gamma$ esu	$Im\chi^{(3)}$ m^2/V^2	$Re\chi^{(3)}$ m^2/V^2
PVA matrix	+3.0	5.52×10^{-14}	1.238×10^{-11}	0.29×10^{-22}	1.63×10^{-20}
1 wt% doped PVA	−1.55	-2.85×10^{-14}	-0.743×10^{-11}	4.36×10^{-22}	3.15×10^{-20}

case of pure and doped PVA, the distance between peak and valley is observed to be 10.50 and 10.21 mm which is closer to the condition of third-order nonlinearity ($1.7z_R = 10.35$ mm). Also, in NLO processes of thermal origin, usually ΔZ_{p-v} will be greater than $1.7z_R$. $\Delta Z_{p-v} = 1.7z_R$ indicate that the optical nonlinearity calculated here is not of thermal origin but predominantly from electronic in nature [41].

4. Conclusions

The PVA films doped with different concentration of 4N4MSP were investigated for their structural, linear optical and nonlinear optical property studies. In the doped films there were significant changes in the molecular bonding leading to CTC as evident from FTIR studies. UV–Visible spectrum reveals there is a red shift in the absorption peak in the visible region with the increase in dopant concentration from 0.1 wt % to 1 wt%. Pure PVA has the optical bandgap of about 5eV, but as the dopant concentration increases the band gap decreases to about 2eV. Refractive index of the dielectric medium increases with the dopant concentration results in the increase of dielectric losses. From powder XRD spectrum it is observed that crystallinity of the medium decreases with increasing dopant concentration. Fluorescence study reveals that fluorescence peak intensity increases up to 0.5 wt% and then decreases for higher concentration. The nonlinear absorption and refraction studies through z-scan technique confirm the superior third order nonlinear efficiency when compared with reported literature data. The dopant concentration of 4N4MSP has its clear role in the enhancement of carrier charge mobility, decreasing the width of the band gaps energies, excellent fluorescence emission peaks in the visible region and in increasing the molecular polarization of the host material. For these reasons, 4N4MSP-PVA composites are suggested as an excellent material to be explored in the opto-electronic devices, especially in solar cell applications.

Declaration of competing interest

The authors declare that they have no known competing financial interests or personal relationships that could have appeared to influence the work reported in this paper.

CRediT authorship contribution statement

E. Deepak D'Silva: Conceptualization, Methodology, Investigation, Writing - original draft, Funding acquisition, Formal analysis. **Ismayil:** Visualization, Validation, Resources, Formal analysis. **Anshu Gaur:** Visualization, Software, Data curation. **S. Venugopal Rao:** Validation, Resources, Writing - review & editing.

Acknowledgments

The authors thank the Director, Sophisticated Test and Instrumentation Centre, Cochin for experimental facilities. One of the authors E Deepak D'Silva is grateful to Vision Group on Science and Technology (VGST), Government of Karnataka, India; for the financial support through the project GRD No. 688. S. Venugopal Rao thanks DRDO for continuous financial support through ACRHEM.

References

[1] T. Huang, Z. Hao, H. Gong, Z. Liu, S. Xiao, S. Li, Y. Zhai, S. You, Q. Wang, J. Qin, Third-order nonlinear optical properties of a new copper coordination compound: a promising candidate for all-optical switching, Chem. Phys. Lett. 451 (2008) 213–217.

[2] K. Satoh, Poly(vinyl Alcohol) (PVA). Encyclopedia of Polymeric Nanomaterials. Springer-Verlag, Berlin, Heidelberg, 2014, https://doi.org/10.1007/978-3-642-36199-9_246-1.

[3] B.M. Baraker, B. Lobo, Dispersion parameters of cadmium chloride doped PVA-PVP blend films, J. Polym. Res. 24 (5) (2017).

[4] M. Jiang, J. Zhu, C. Chen, Y. Lu, Y. Ge, X. Zhang, Poly(vinyl alcohol) borate gel polymer electrolytes prepared by electrodeposition and their application in electrochemical supercapacitors, ACS Appl. Mater. Interfaces 8 (5) (2016) 3473–3481.

[5] P. Balaji Bhargav, V. Madhu Mohan, A.K. Sharma, V.V.R.N. Rao, Investigations on electrical properties of (PVA: NaF) polymer electrolytes for electrochemical cell applications, Curr. Appl. Phys. 9 (1) (2009) 165–171.

[6] T.S. Gaaz, A.B. Sulong, M.N. Akhtar, A.A.H. Kadhum, A.B. Mohamad, A.A. Al-Amiery, Properties and applications of polyvinyl alcohol, halloysite nanotubes and their nanocomposites, Molecules 20 (2015) 22833–22847.

[7] A.M. Bagher, M.M.A. Vahid, M. Mohsen, Types of solar cells and application, Am. J. Optic. Photon. 3 (5) (2015) 94–113.

[8] R. Kroon, M. Lenes, J.C. Hummelen, P.W.M. Blom, B. de Boer, Small bandgap polymers for organic solar cells (polymer material development in the last 5 years), Polym. Rev. 48 (3) (2008).

[9] S. Muhammad, A.G. Al-Sehemi, M. Pannipara, A. Irfan, Design, characterization and nonlinear optical properties of coumarin appended chalcones: use of a dual approach, Optik 164 (2018) 5–15.

[10] M. Sai Kiran, Benoy Anand, S. Siva Sankara Sai, G. Nageswara Rao, Second- and third-order nonlinear optical properties of bis-chalcone derivatives, J. Photochem. Photobiol., A: Chem. 290 (2014) 38–42.

[11] P. Poornesh, S. Shettigar, G. Umesh, K.B. Manjunatha, K. Prakash Kamath, B. K. Sarojini, B. Narayana, Nonlinear optical studies on 1,3-disubstituent chalcones doped polymer films, Opt. Mater. 31 (2009) 854–859.

[12] E.D. D'silva, G. Krishna Podagatlapalli, S. Venugopal Rao, S.M. Dharmaprakash, Structural, optical and electrical characteristics of a new NLO crystal, Optic Laser. Technol. 44 (6) (2012) 1689–1697.

[13] E.D. D'silva, D. Narayana Rao, Reji Philip, Ray J. Butcher, Rajnikant, S. M. Dharmaprakash, Synthesis, growth and characterization of novel second harmonic nonlinear chalcone crystal, J. Phys. Chem. Solid. 72 (2011) 824–830.

[14] R.F. Bhajantri, V. Ravindrachary, A. Harisha, Vincent Crasta, S.P. Nayak, Boja Poojary, Microstructural studies on BaCl2 doped poly(vinyl alcohol), Polymer 47 (10) (2006) 3591–3598.

[15] K. Janardhana, V. Ravindrachary, P.C. Rajesh Kumar, Ismayil, Investigation of third-order nonlinear optical properties of pyrazoline-doped polyvinyl alcohol films, Polym. Eng. Sci. 53 (2013) 1958–1967.

[16] F. Yakuphanoglu, M. Arslan, Determination of electrical conduction mechanism and optical band gap of a new charge transfer complex: TCNQ-PANT, Solid State Commun. 132 (3–4) (2004) 229–234.

[17] F. Yakuphanoglu, M. Sekerci, A. Balaban, The effect of film thickness on the optical absorption edge and optical constants of the Cr (III) organic thin films,, Opt. Mater. 27 (2005) 1369–1372.

[18] I. Saleem Qashou, Methylsilicon phthalocyanine hydroxide doped PVA films for optoelectronic applications: FTIR spectroscopy, electrical conductivity, linear and nonlinear optical studies, Phys. B Condens. Matter 571 (2019) 93–100. E.F.M. El-Zaidia. A.A.A. Darwish. T.A. Hanafy.

[19] F. Urbach, The long-wavelength edge of photographic sensitivity and of the electronic absorption of solids,, Phys. Rev. 92 (1953) 1324.

[20] E.A. Davis, N. Mott, Conduction in non-crystalline systems V. Conductivity, optical absorption and photoconductivity in amorphous semiconductors, Philos. Mag. A 22 (179) (1970) 903–922.

[21] N. Xie, Y. Chen, Construction and photoswitching properties of fluorescent diarylethenes, J. Mater. Chem. 17 (9) (2007) 861.

[22] F.F. Muhammad, S.B. Aziz, S.A. Hussein, Effect of the dopant salt on the optical parameters of PVA: $NaNO_3$ solid polymer electrolyte, J. Mater. Sci. Mater. Electron. 26 (1) (2015) 521–529.

[23] F. Yakuphanoglu, M. Kandaz, M.N. Yarasir, F.B. Senkal, Electrical transport and optical properties of an organic semiconductor based on phthalocyanine, Phys. B 393 (1–2) (2007) 235–238.

[24] N.A. Bakr, A.M. Funde, V.S. Waman, M.M. Kamble, R.R. Hawaldar, D. P. Amalnerkar, S. Gosavi, S.R. Jadkar, Determination of the optical parameters of a-Si:H thin films deposited by hot wire–chemical vapour deposition technique using transmission spectrum only, Pramana - J. Phys. 76 (2011) 519–531.

[25] F. Yakuphanoglu, M. Sekerci, O.F. Ozturk, The determination of the optical constants of Cu(II) compound having 1-chloro-2,3-o-cyclohexylidinepropane thin film, Opt, Commun. Now. 239 (2004) 275–280.

[26] F.F. Muhammad, K. Sulaiman, Utilizing a simple and reliable method to investigate the optical functions of small molecular organic films – Alq3 and Gaq3 as examples, Measurement 44 (2011) 1468–1474.

[27] V. Ravindrachary, R.F. Bhajantri, A. Harisha, Ismayil, C. Ranganathaiah, Microstructure and positron behavior in $FeCl_3$ doped PVA/PVP blend, Phys. Status Solidi C 6 (2009) 2438–2441.

[28] H.M. Zidan, Structural properties of CrF_3- and $MnCl_2$-filled poly(vinyl alcohol) films, J. Appl. Polym. Sci. 88 (2003) 1115–1120.

[29] B. Ian Burgess, P. Rochon, N. Cunningham, Photophysical properties of commercial red dyes in polymer films, Opt. Mater. 30 (2008) 1478–1483.

[30] M.-L. Wang, J.-Z. Liu, C.-X. Xu, Intra molecular charge transfer in arylpyrazolines, Chin. Phys. Lett. 23 (2006) 3088–3090.

[31] R.F. Bhajantri, V. Ravindrachary, B. Poojary, A. Ismayil, V. Crasta Harisha, Studies on fluorescent PVA+PVP+MPDMAPP, composite films, Polym. Eng. Sci. 49 (2009) 903.

[32] F.M. Zehentbauer, C. Moretto, R. Stephen, T. Thevar, J.R. Gilchrist, D. Pokrajac, K. L. Richard, J. Kiefer, Fluorescence spectroscopy of rhodamine 6G: concentration and solvent effects, spectrochim, Acta Part A: Mol. Biomol. Spectrosc 121 (2014) 147–151.

[33] M. Sheik-Bahae, A.A. Said, T.H. Wei, D.J. Hagan, E.W. Van Stryland, Sensitive Measurement of optical nonlinearities using a single beam, J. Quant. Econ. 26 (1990) 760.
[34] S. Qi, C. Zhang, X. Yang, K. Chen, L. Zhang, G. Yang, X. Liang, T. Xu, J. Tian, s Absorption characteristic and limiting effect of Congo red doped PVA film, Opt. Mater. 29 (2007) 1348–1351.
[35] A. Gaur, H. Syed, B. Yendeti, Venugopal Rao Soma, Experimental evidence of two-photon absorption and its saturation in malachite green oxalate: a femtosecond Z-scan study, J. Opt. Soc. Am. B 35 (2018) 2906.
[36] N. Dong, Y. Li, S. Zhang, N. McEvoy, R. Gatensby, G.S. Duesbergand, J. Wang, Saturation of two-photon absorption in layered transition metal dichalcogenides: experiment and theory, ACS Photonics 5 (2018) 1558–1565.
[37] M. Sean Kirkpatrick, R. Rajesh Naik, O. Morley Stone, Nonlinear saturation and determination of the two-photon absorption cross section of green fluorescent protein, J. Phys. Chem. B 105 (2001) 2867–2873.
[38] B. Gu, J. He, W. Ji, H.-T. Wang, Three-photon absorption saturation in ZnO and ZnS crystals, J. Appl. Phys. 103 (2008), 073105.
[39] P.C. Rajesh Kumara, K. Janardhana, K.M. Balakrishna, T. Sheela, Study of nonlinear optical properties of a chalcone doped PVA composite material, Procedia Eng. 141 (2016) 83–90.
[40] E.D. D'Silva, G. Krishna Podagatlapalli, S. Venugopal Rao, S.M. Dharmaprakash, Study on third-order nonlinear optical properties of 4-methylsulfanyl chalcone derivatives using picosecond pulses, Mater. Res. Bull. 47 (2012) 3552–3557.
[41] K. Janardhana, V. Ravindrachary, P.C. Rajesh Kumar, Ismayil, Investigation of third-order nonlinear optical properties of pyrazoline-doped polyvinyl alcohol films, Polym. Eng. Sci. 53 (2013) 1958–1967.